

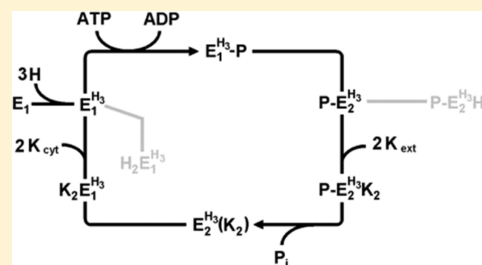
Role of Protons in the Pump Cycle of KdpFABC Investigated by Time-Resolved Kinetic Experiments

Bojana Damjanovic^{†,‡} and Hans-Jürgen Apell^{*,†,‡}

[†]Department of Biology, University of Konstanz, 78464 Konstanz, Germany

[‡]Konstanz Research School of Chemical Biology, University of Konstanz, 78464 Konstanz, Germany

ABSTRACT: The time-resolved kinetics of the KdpFABC complex solubilized in Aminoxide WS-35 was investigated by ATP concentration jump experiments. ATP was photoreleased from its inactive precursor, caged ATP, and charge movements in the membrane domain of the KdpFABC were detected by the electrochromic dye RH421. At low ATP concentrations, the ATP binding step became rate-limiting with an apparent, pH-independent ATP binding affinity of $\sim 70 \mu\text{M}$. At saturating ATP concentrations, the rate-limiting step is the conformational transition ($E_1\text{--P} \rightarrow \text{P--}E_2$) with a rate constant of $\sim 1.7 \text{ s}^{-1}$ at 20°C that was independent of K^+ concentration. This observation together with the detected fluorescence decrease indicates that K^+ (or another positive ion) is bound in the membrane domain after enzyme phosphorylation and the conformational transition to the $\text{P--}E_2$ state. pH dependence experiments revealed different roles of H^+ in the transport mechanism. Two different functions of protons for the ion pump must be distinguished. On one hand, there are electrogenically bound “functional” protons, which are not transported but prerequisite for the performance of the ATP-driven half-cycle. On the other hand, protons bind to the transport sites, acting as weak congeners of K^+ . There possibly are noncompetitively bound protons, affecting the enzyme activity and/or coupling between KdpA and KdpB subunits. Finally, the recently proposed Post-Albers model for the KdpFABC complex was supplemented with stoichiometry factors of 2 for K^+ and 3 for H^+ , and additional inhibitory side reactions controlled by H^+ were introduced, which are relevant at $\text{pH} < 6.5$ and/or in the absence of K^+ .



On gradients across cellular membranes underlie a large variety of vital biochemical functions. Therefore, nature has developed sophisticated transport nanomachines in all kingdoms of life to maintain the required gradients of the respective electrochemical potentials. A major class of ion pumps, the P-type ATPases, is present in virtually all living cells, and these ion pumps are involved in transporting cations across biological membranes at the expense of ATP.^{1,2} Most of the knowledge of P-type ATPases was obtained from detailed studies of eukaryotic P-type ATPases. Important contributions were provided by the elucidation of the structure of the sarcoplasmic reticulum Ca-ATPase (SERCA) at various stages of the reaction cycle.^{3–6} Members of the P-type ATPase superfamily generally consist of a single subunit with a molecular mass between 70 and 150 kDa that mediates both ATP hydrolysis and ion binding and transport. In contrast to the well-studied and mutually related eukaryotic P-type ATPases, much less is known about their bacterial homologues. An example of rather unusual prokaryotic P-type ATPase is the KdpFABC complex of *Escherichia coli*.

Potassium is the most abundant monovalent cation in the cytoplasmic compartment of *E. coli* and is essentially involved in pH homeostasis, in turgor maintenance, and in the activation of various enzymes. For these reasons, *E. coli* has developed a set of well-defined and highly specialized K^+ uptake systems. Among these, the KdpFABC complex is an inducible, high-affinity potassium uptake system, expressed only when the other K^+ -scavenging systems, including KtrAB, Kup, and Trk,

cannot meet the needs of the cells for potassium. In contrast to other closely related eukaryotic P-type ATPases, the KdpFABC complex is rather unique because it is composed of four subunits, and ion transport (KdpA) and ATP hydrolysis (KdpB) are spatially separated on two different polypeptides (Figure 1A).

The largest subunit, KdpB (72 kDa), comprises all the signature motifs and properties of the P-type ATPase family, including the four distinct characteristic domains, the phosphorylation (P), nucleotide binding (N), actuator (A), and membrane (M) domains.⁷ The KdpA subunit (59 kDa) shows similarities to KcsA-like K^+ channel proteins and is known to be the ion-translocating subunit.^{8,9} Despite the observed structural similarities between the KdpA and potassium channels, the underlying ion transport mechanisms are fundamentally different. Whereas KcsA channels allow passive diffusion of K^+ ions across the membranes, the KdpA subunit mediates the uphill movement of ions utilizing the energy released during ATP hydrolysis. The energy derived from ATP hydrolysis in the KdpB subunit is transferred to the site(s) of ion translocation within the KdpA subunit via a coupling mechanism that involves two conserved charged residues, D583 and K586, located in the transmembrane

Received: March 19, 2014

Revised: April 24, 2014

Published: April 25, 2014



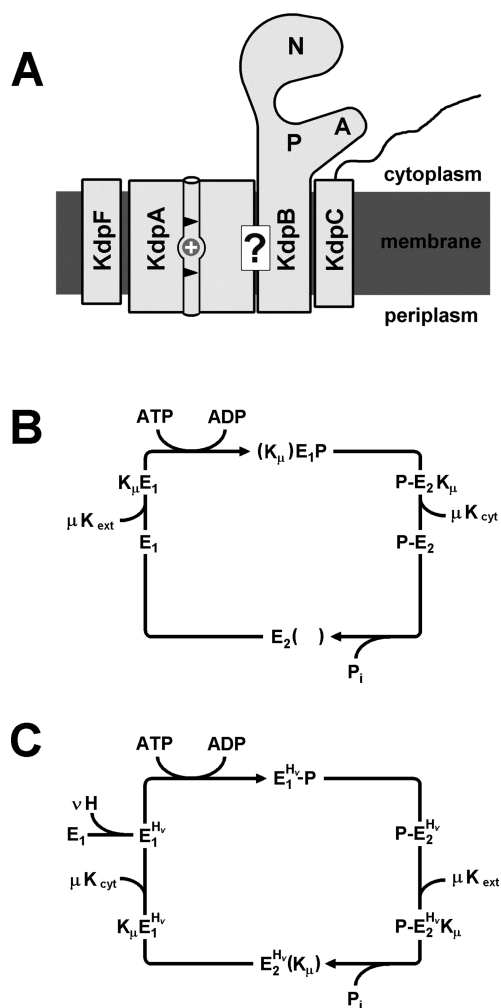


Figure 1. Schematic drawing of the KdpFABC complex and proposed Post-Albers models, adapted from refs 14 and 18. (A) The still unknown mechanism of coupling among the KdpB subunit, a P-type ATPase, and the KdpA subunit that resembles a bacterial K^+ channel permits the uphill transport of K^+ . The major functional domains of KdpB, -N, -P, and -A, characteristic of P-type ATPases, are denoted.⁷ (B) Proposal of a model that places K^+ transport in the ATP-driven half-cycle, with no other ion species being involved in the reaction cycle (according to Bramkamp and Altendorf¹⁴). (C) Alternative model, derived from the more “classical” scheme valid for type II P-type ATPases, such as the Na,K-ATPase, suggesting that K^+ transport occurs in the dephosphorylation cycle, whereas the presence of ν -protons inside the membrane domain is a prerequisite for the ATP-driven half-cycle. Protons are not translocated but remain “occluded” in the sites throughout the whole reaction cycle. They are indicated by the superscript “H ν ”. ν and μ are stoichiometric factors.

domain of the KdpB subunit.¹⁰ Investigations of the KdpC (21 kDa) subunit indicate a regulatory function,^{11,12} similar to that of phospholamban or calmodulin, or the γ subunit of the Na,K-ATPase, although it shows no homology to any other known protein. The functional unit of the KdpFABC complex is a homodimer with two adjacent KdpFABC complexes interacting via their neighboring KdpB subunits. Subunit interactions are stabilized by the smallest subunit, KdpF (3 kDa), correspondingly termed molecular glue, which can be replaced by a large amount of *E. coli* lipids *in vitro*.¹³

It is well-known that the P-type ATPases exist in two major conformations and catalytic states named E_1 and E_2 . Large

domain movements between both states are triggered by reversible phosphorylation of a highly conserved aspartate residue, resulting in altered binding affinities for both ATP and the transported ion species. The reaction cycle is schematically represented with a so-called Post-Albers model, which is the generally accepted pump cycle for all members of the P-type ATPase family. Two models for the KdpFABC reaction cycle were proposed so far. According to the one introduced by Bramkamp and Altendorf, K^+ transport takes place in the ATP-driven half-cycle while no ions are translocated in the subsequent dephosphorylation half-cycle.¹⁴ In this proposal, the transport direction in the ATP-driven half-cycle is reversed with respect to the pump mode of type II P-type ATPases (Figure 1B), and it does not consider the role of protons, which were shown to interact in at least two different ways. The first is the function of a weak congener of K^+ . Protons can be transported with low efficiency in the absence of K^+ , similar to what has been already observed for Rb^+ , Na^+ , and Li^+ .^{15–17} The second function of protons is noncompetitive binding. It was shown that H^+ binding is an electrogenic process, not significantly affected by the presence of K^+ , and these ion binding sites may be located on the KdpA or KdpB subunit.¹⁸ To account also for the role of protons, a model was recently proposed that is adapted from the “classical” Post-Albers cycle in which K^+ is transported during the dephosphorylation half cycle.¹⁸ This model includes protons, which remain occluded in specific “functional sites” throughout the whole reaction cycle, and their binding inside the membrane domain is a prerequisite for the ATP-driven half-cycle. To discriminate clearly between such functional protons and those transported as congeners of K^+ , we denote them as superscripts to the respective conformational states (Figure 1C).

In this work, time-resolved experiments provided additional details about the transport kinetics that allow refinement of the proposed reaction mechanism. The fluorescent dye RH421 monitors ion binding and release reactions in the submillisecond time range,¹⁹ and caged ATP was used to produce ATP concentration jumps that trigger the enzyme phosphorylation-induced partial reaction. Caged ATP is a photolabile ATP precursor that releases ATP in 1–5 ms upon a UV light flash²⁰ and thus allows investigation of reaction steps of the KdpFABC complex with time constants of >10 ms. The styryl dye RH421 has been used previously to investigate the electrogenicity of ion binding partial reactions of the pump cycle of the detergent-solubilized KdpFABC in steady-state titration experiments.¹⁸ Here, the kinetics of the conformational transition is investigated in the presence of saturating ATP concentrations, and the effects of different K^+ concentrations, pHs, and temperatures are studied. The apparent ATP binding affinity of the detergent-solubilized enzyme is obtained, and activation energies of detergent-solubilized KdpFABC are determined both by time-resolved measurements and by the malachite green activity assay.

MATERIALS AND METHODS

Materials. The electrochromic styryl dye RH421 was ordered from MoBiTec and NPE-caged ATP (disodium salt) from Molecular Probes. ATP (disodium salt, special quality) was obtained from Roche. β -DDM was purchased from Anatrace (Maumee, OH). All other reagents were purchased from Merck or Sigma-Aldrich at the highest quality available.

Expression and Purification of the KdpFABC Complex. The KdpFABC complex was expressed in *E. coli* as described

previously.^{18,21,22} In short, a His₁₄ tag was added to the C-terminus of the KdpA subunit before its expression in *E. coli*. Cells were adapted to extremely low potassium concentrations promoting KdpFABC expression during a period of 3 days. The protein expression was achieved by additions of KCl at time points at which the level of cell growth reached a plateau. Finally, cells were harvested by centrifugation at an optical density of ~ 1 at 600 nm, and cell pellets were flash-frozen in liquid nitrogen and stored at -80°C . Cells were lysed with a French press, and membranes containing the KdpFABC complex were harvested as the supernatant by low-speed centrifugation (10000g for 15 min) followed by centrifugation at 200000g and 4°C for 60 min. The pellet that was resuspended in 50 mM Tris-HCl (pH 7.5), 10 mM MgCl₂, 10% (v/v) glycerol, 1 mM DTT, and 0.5 mM PMSF at a protein concentration of 5 mg/mL, and KdpFABC complexes were solubilized using 1% (w/v) AminoXide WS-35 (Goldschmidt) for 60 min on ice with gentle stirring. The solubilized protein was collected by centrifugation as the supernatant and bound to a 5 mL HisTrap column (GE Healthcare). The column was connected to a FPLC system (Amersham, Biotech) and washed with 50 mM Tris-HCl, 20 mM MgCl₂, 10% (v/v) glycerol, 150 mM NaCl, 20 mM imidazole (pH 7.5), 0.5 mM PMSF, and 0.2% (w/v) AminoXide WS-35 at a flow rate of 0.5 mL/min. Thereafter, the enzyme was eluted with the same buffer containing 130 mM imidazole. Samples of the protein-containing fractions were analyzed on a 12.5% sodium dodecyl sulfate–polyacrylamide gel electrophoresis (SDS–PAGE) gel. Fractions containing the KdpFABC complex were further collected and concentrated to a volume of 500 μL . Finally, the protein solution was loaded on a Superdex 200 column (GE Healthcare) and eluted with 50 mM Tris-HCl (pH 7.5), 150 mM NaCl, 0.5 mM PMSF, and 0.2% (w/v) AminoXide WS-35 at a flow rate of 0.5 mL/min. Fractions containing the purified complexes were concentrated as described above. The integrity of their subunit composition was checked by SDS–PAGE. Alternatively, the KdpFABC complexes were solubilized using 1% (w/v) β -DDM for 1 h on ice and purified using the same buffers containing 0.2% (w/v) β -DDM.

Determination of the Protein Concentration and ATPase Activity. The protein concentration in membrane vesicles was determined by use of the bicinchoninic acid assay (Pierce) according to the manufacturer's protocol. The concentration of detergent-solubilized protein was determined by the Lowry assay. ATPase activities of purified complexes were determined at 37°C using the malachite green activity assay.^{18,23} The ATPase activity of the KdpFABC complex solubilized in AminoXide WS-35 was $0.87 \pm 0.02 \mu\text{mol of P}_i$ (mg of protein)⁻¹ min⁻¹ at 37°C in the presence of 3.3 mM KCl (pH 7.8). The total amount of protein needed for a single measurement was $\sim 1 \mu\text{g}$.

Measurement of Transient RH421 Fluorescence Signals. The kinetic experiments with detergent-solubilized KdpFABC were performed with a homemade setup as described in principle previously.^{24,25} The photochemical release of ATP was triggered by a UV flash generated by an EMG 100 excimer laser (Lambda Physics, Göttingen, Germany; wavelength of 351 nm, duration of 14 ns, power of 3.5 MW). At pH 7.0, ATP is released from caged ATP with a time constant of 4.6 ms.²⁰ A UV cutoff filter in front of the photomultiplier entrance window was used to reduce the effect of the UV flash on the photomultiplier. RH421 was excited with a HeNe laser working at 594 nm. A quartz lens widens the

laser beam to illuminate the whole solution homogeneously. The emitted light was collected by an ellipsoidal mirror and converged onto the cathode of a photomultiplier (model R928, Hamamatsu Photonics). A $663 \pm 18 \text{ nm}$ interference filter selects the emitted light of the styryl dye before it enters the photomultiplier. The output current is amplified and digitized by a 12-bit data acquisition board of a personal computer with sampling frequencies between 1 and 100 kHz. The bottom of the cuvette is in contact with a thermostated copper socket that also blocks the incident light. The experiments were performed in a darkened environment at $25 \pm 1^{\circ}\text{C}$, unless stated otherwise. A cylindrical quartz cuvette (internal diameter of 7.8 mm) is filled with 300 μL of buffer containing 25 mM imidazole, 1 mM EDTA (pH 7.8), 5 mM MgCl₂, 200 nM RH421, 9 $\mu\text{g/mL}$ detergent-solubilized KdpFABC, 300 μM caged ATP, and various concentrations of KCl. To remove traces of free ATP from the caged ATP sample, Apyrase VI (1.4×10^{-3} unit/mL) and 1.4 mM MgCl₂ were added to the 10 mM stock solution. Aliquots of caged ATP were flash-frozen in liquid N₂ and stored at -20°C . During the experiments, caged ATP was kept on ice and protected from light. The cuvette was equilibrated for 10–15 min inside the instrument in the dark (to prevent photolysis of caged ATP). After equilibration, the shutter was opened and the experiment was triggered by a UV light flash. The concentration of released ATP was determined by the luciferin/luciferase test that was calibrated using solutions with known ATP concentrations.²⁶ The substrate-dependent change in fluorescence upon ATP release, F_{norm} , was fit by use of the Hill function

$$F_{\text{norm}}([X^+]) = F_0 + \Delta F_{\text{max}}/[1 + ([X^+]/K_{1/2})^{-n}] \quad (1)$$

where $[X^+]$ is the substrate concentration, F_0 the fluorescence level before the flash, ΔF_{max} the maximal fluorescence change, $K_{1/2}$ the half-saturating concentration, and n the Hill coefficient.

RESULTS

Time-Resolved RH421 Fluorescence Signals after an ATP Concentration Jump. Besides the ion binding studies, the electrochromic dye RH421 can be used in time-resolved kinetic experiments, employing caged ATP as a photolabile ATP precursor.^{20,27,28} It allows kinetic studies in biological systems, in which limitations arising from the difficulty of adding the substrate to the system in a time shorter than the reaction time have to be overcome. When the enzyme is phosphorylated after the release of ATP, it undergoes a conformational transition from the E_1 state to the $P-E_2$ state. At high ATP concentrations, ATP binding and enzyme phosphorylation are fast compared to the subsequent conformational transition to the $P-E_2$ state, by which the ion binding sites are exposed to the extracellular side of the membrane, and K^+ ions are able to enter and bind in a diffusion-controlled manner. Thus, the rate constant of the fluorescence change reflects the rate of the $E_1^H-P \rightarrow P-E_2^H$ conformational transition (Figure 1C). Recently, it has been shown that the ATP-induced partial reaction in the absence of K^+ does not produce a significant change in RH421 fluorescence.¹⁸ In the presence of K^+ , the fluorescence decrease detected upon ATP release is an electrogenic reaction due to fast K^+ binding from the extracellular side. The fluorescence trace shown in Figure 2A represents an experiment in the presence of saturating 100 μM K^+ at pH 7.8 and could be fit with a single-exponential function:

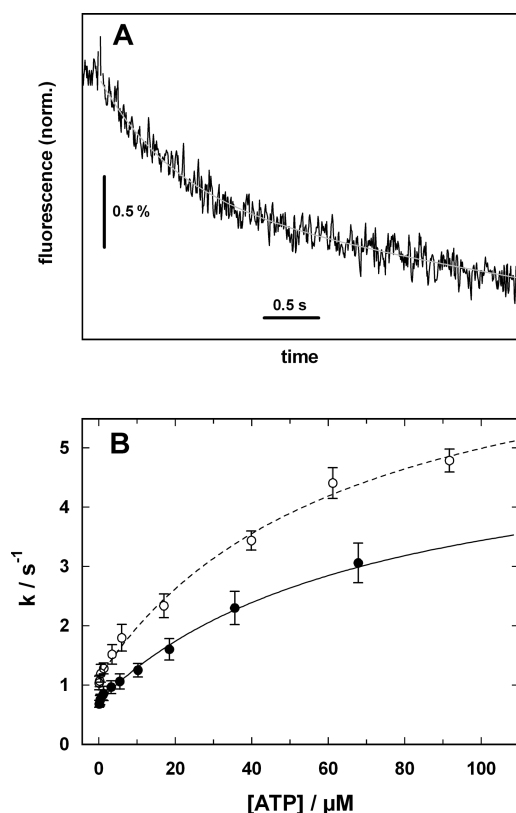


Figure 2. Analysis of time-resolved RH421 fluorescence signals of ATP-induced K^+ binding by KdpFABC. (A) Time course of the fluorescence relaxation after an ATP concentration jump performed with KdpFABC complexes solubilized in Aminoxide WS-35, in the presence of 100 μM K^+ at pH 7.8 and 25 ± 1 °C. The experimental data were fit with the single-exponential function, as shown by the gray line. (B) Concentration dependence of the rate constant, k , of the fluorescence decrease in the presence of ATP concentrations released from different (nonsaturating) amounts of caged ATP in the presence of saturating 100 μM KCl. The apparent ATP binding constant was determined from the fitted Michaelis–Menten curve to be 72 ± 7 μM at pH 7.8 (●) and 65 ± 17 μM at pH 6.1 (○).

$$F_{\text{norm}}(t) = A(1 - e^{-kt}) \quad (2)$$

where k is the rate constant of the fluorescence decrease after ATP release. The observation that the fluorescence trace could be fit with a single-exponential function indicates that the ATP-induced partial reaction is rate-limited by a single reaction step.

ATP Concentration Dependence. When the ATP concentration is saturating, the rate-limiting step in the ATP-induced reaction sequence is the conformational transition, from E_1 to E_2 . At low ATP concentrations, however, ATP binding becomes rate-limiting and, therefore, affects the time course of the fluorescence response. Under this condition, it is possible to determine the apparent ATP binding constant of the detergent-solubilized KdpFABC complex from the ATP concentration dependence of the rate constant, k , of the fluorescence decrease in the presence of saturating 100 μM KCl (Figure 2B). Experiments were performed with various ATP concentrations at pH 7.8 and 6.1 to investigate the effect of protons on ATP binding affinity and to reveal their role specifically in the phosphorylation step. The concentration of caged ATP was varied between 1 and 400 μM , and a luciferin/luciferase assay was used to determine the effective ATP concentration after the photochemical release. The recorded

fluorescence decrease was fit with a single-exponential function (eq 2), and the resulting rate constants were plotted against the respective ATP concentrations (Figure 2B). The apparent ATP binding affinity at pH 7.8 was determined using a Michaelis–Menten function. A half-saturating concentration, $K_{1/2}$, of 72 ± 7 μM was found with a maximal k of 5.4 ± 0.2 s⁻¹ (solid line). At pH 6.1, the apparent ATP affinity was not significantly different with a $K_{1/2}$ of 65 ± 17 μM (dashed line). Both $K_{1/2}$ values agree with the ATP binding affinity determined by measurements of the enzyme activity under comparable conditions.¹⁸ The maximal k of 7.5 ± 0.7 s⁻¹ was enhanced at pH 6.1. This finding indicates that the presence of higher proton concentrations accelerates the rate-limiting reaction step. Concentrations of caged ATP of >400 μM were not applied because of possible artifacts caused by the strong absorption of the caged ATP that prevents a homogeneous illumination by the UV flash and, therefore, a homogeneous release of ATP. Moreover, in previously published work, the inhibition constant of caged ATP for the KdpFABC complex was determined to be 630 μM in the presence of a saturating K^+ concentration, indicating that caged ATP acts as a weak competitive inhibitor of ATP binding.²⁹

K^+ Concentration Dependence. Similar sets of experiments were performed in the presence of various K^+ concentrations between 0.1 and 500 μM at pH 7.8 and 25 ± 1 °C. For each concentration, at least three measurements were performed. The average rate constants were calculated and plotted against the respective K^+ concentrations (Figure 3).

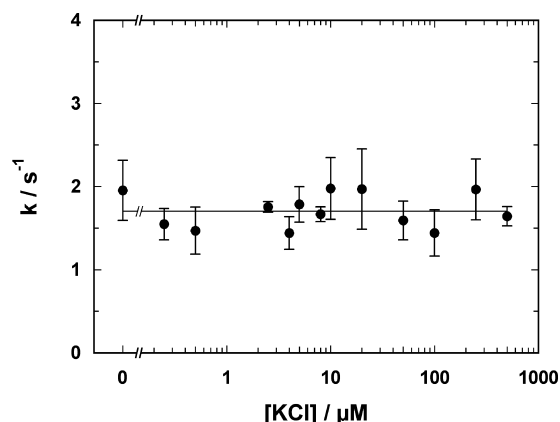


Figure 3. Dependence of the rate constant, k , on K^+ concentration. The fluorescence decrease (as in Figure 2A) was triggered by the ATP release from 300 μM caged ATP at pH 7.8 and 25 ± 1 °C. No significant concentration dependence was obtained, with an average rate constant, k , of 1.7 ± 0.1 s⁻¹.

The obtained results show that the detected rate constant does not depend on the K^+ concentration, and its average value was found to be 1.7 ± 0.1 s⁻¹. This finding indicates that the rate constant of the rate-limiting process is not significantly dependent on the K^+ concentration, even at concentrations far below the corresponding $K_{1/2}$ value of K^+ binding (6.5 μM) and in the absence of K^+ . This rate constant reflects the turnover rate of the pump cycle in these experiments. It is worth mentioning that the determined rate constant of 1.7 s⁻¹ is 100-fold smaller than the rate of the UV flash-induced ATP release reaction (see below), and therefore, the observed fluorescence decrease is not affected by the ATP release kinetics.

In contrast, the absolute values of the maximal fluorescence amplitude showed a significant increase with increasing K^+ concentrations (Figure 4A). The data were fit with a Hill

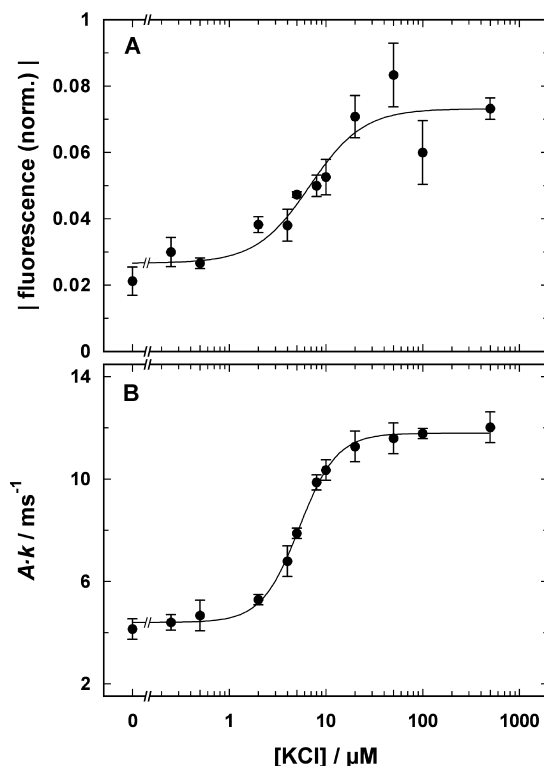


Figure 4. Analysis of the RH421 fluorescence signals in the presence of various K^+ concentrations at pH 7.8 and 25 ± 1 °C. For each measurement, 300 μM caged ATP was used, and data result from fits to the average of three independent experiments (\pm the standard error of the mean). (A) K^+ dependence of the absolute value of the fluorescence decrease, A , fit with the Hill function (eq 1). The half-saturating K^+ concentration, $K_{1/2}$, was found to be 6.8 ± 2.0 μM and the Hill coefficient, n , to be 1.8 ± 0.8 . (B) Dependence of the initial slope of the fluorescence decrease determined as a product of the amplitude, A , and the rate constant, k , obtained from the fit of the fluorescence decrease by a monoexponential function. The fit with the Hill function resulted in a $K_{1/2}$ of 5.27 ± 0.24 μM and an n of 2.3 ± 0.2 .

function (eq 1), and the half-saturating K^+ concentration, $K_{1/2}$, was found to be 6.8 ± 2.0 μM with a Hill coefficient, n , of 1.8 ± 0.8 , indicating a cooperative binding of more than one K^+ . The obtained $K_{1/2}$ is in agreement with previously published values under physiological conditions,^{30,31} and from equilibrium titration experiments with solubilized KdpFABC complexes.¹⁸

A more accurate analysis is shown in Figure 4B. The initial slope of the fluorescence change upon the ATP concentration jump is proportional to both the number of pumps activated by ATP and the rate of the limiting reaction step that is reflected by the rate constant k .²⁵ The initial slope of the fluorescence decrease can be calculated as the first derivative of the single-exponential function (eq 2) at time zero:

$$\left[\frac{dF_{\text{norm}}(t)}{dt} \right]_{t=0} = \Delta F_{\text{max}}(-k)e^{-kt}|_{t=0} = -\Delta F_{\text{max}}k = f_{\text{max}}N_p k \quad (3)$$

Taking this approximation into account, the product of the absolute value of the amplitude of the fluorescence decrease,

$|\Delta F_{\text{max}}|$, and the corresponding rate constant, both taken from the fits to the data, were calculated and plotted against the respective K^+ concentrations (Figure 4B). f_{max} is the contribution of a single (active) pump to the fluorescence signal, and N_p is the number of pumps contributing by ATP activation. The K^+ concentration dependence was fit with a Hill function (eq 1), providing a half-saturating K^+ concentration, $K_{1/2}$, of 5.27 ± 0.24 μM and a Hill coefficient of 2.3 ± 0.2 . This analysis provided a higher accuracy than the K^+ -dependent amplitude alone (Figure 4A). Because in Figure 3 it has been shown that the rate constant, k , is not dependent on K^+ concentration, obviously, the number of pumps activated by ATP is crucial for the initial slope.

pH Dependence. To further elucidate the role of protons in the reaction cycle of the KdpFABC complex, ATP concentration jump experiments were performed at various pH values to investigate the effects of H^+ on the conformational transition and electrogenic K^+ binding. Experiments were performed between pH 6.15 and 8.6, in the absence and presence of saturating 100 μM K^+ , and in the presence of 300 μM caged ATP, which led to a concentration jump of ~ 40 μM ATP. All experiments were performed at least three times, and the average fluorescence signal was calculated. The fluorescence decrease could be fit with a single-exponential function (eq 2) with an additional minor linear drift component, and the determined rate constants, k , were plotted against the respective pH (Figure 5A). The pH dependence of the rate constants in the absence of K^+ had to be fit by the sum of two Hill functions (solid line), with a pK_1 of 7.4 ± 0.1 and an n_1 of 6.1 ± 0.5 and with a pK_2 of 7.0 ± 0.0 and an n_2 of 4.2 ± 0.4 . The highest rate constant of ~ 5 s^{-1} was found at pH ~ 7.2 . The results obtained in the presence of saturating K^+ were fit with a single Hill function (dashed line), with a pK of 6.7 ± 0.1 and a Hill coefficient of 2.0 ± 1.0 .

The pH dependence of the amplitude of the fluorescence decrease in the absence and presence of saturating K^+ concentration is shown in Figure 5B. In the absence of K^+ , the fluorescence decrease was on the whole pH-independent with a small average amplitude of -0.19 ± 0.01 (solid line). This finding indicates that only a minor net charge movement in the binding sites occurred during the transition from the E_1 state to the $P-E_2$ state. On the other hand, in the presence of saturating 100 μM K^+ , the fluorescence decrease became larger with decreasing H^+ concentrations (dashed line). The respective pK was determined to be 6.8 ± 0.2 , with a Hill coefficient, n , of 1.1 ± 0.4 and a maximal fluorescence amplitude of $-7.8 \pm 0.4\%$. This result indicates that protons are able to prevent a (noncompetitive) binding of K^+ , and possible mechanisms for the observed inhibition will be discussed in detail (see below).

To evaluate the effect of protons on the rate constant of the conformational transition of the KdpFABC complex, a possible artifact produced by the pH-dependent ATP release kinetics has to be discussed. The time dependence of ATP release is given by the equation^{24,32,33}

$$[ATP] = \theta[\text{caged ATP}](1 - e^{-\lambda t}) \quad (4)$$

where $[\text{caged ATP}]$ and $[ATP]$ are the concentrations of caged ATP and released ATP, respectively, θ is the quantum yield of the photoreaction, t is the time, and λ is a characteristic rate constant of the ATP release process that is pH-dependent and has been determined as³⁴

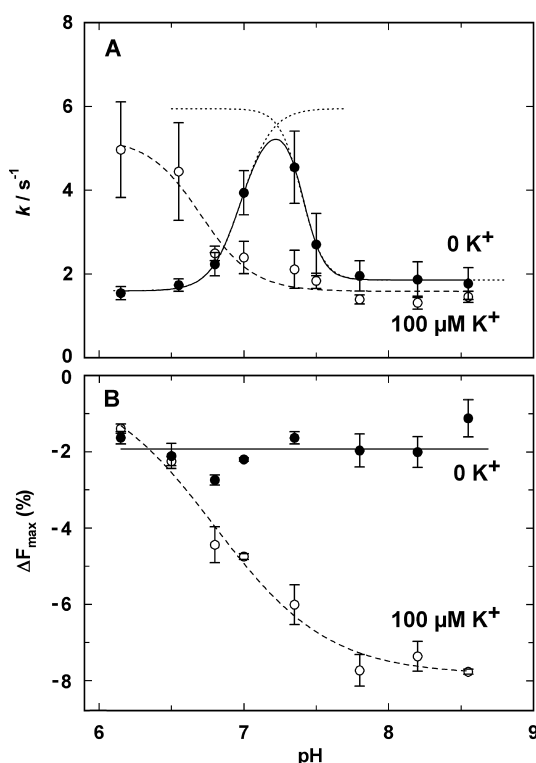


Figure 5. pH dependence of the fluorescence decrease in the absence and presence of 100 μM K⁺ at 25 \pm 1 °C. For each measurement, 300 μM caged ATP was used, and data result from fits to the average of three independent experiments (\pm the standard error of the mean). (A) pH dependence of the rate constants, k , in the absence of K⁺ (●). The data were fit with a sum of two Hill functions with a pK_1 of 7.4 ± 0.1 ($n = 6.1 \pm 0.5$) and a pK_2 of 7.0 ± 0.1 ($n = 4.2 \pm 0.5$). The rate constants in the presence of 100 μM K⁺ (○) were fit with a single Hill function with a pK of 6.7 ± 0.1 ($n = 2.0 \pm 1.0$). (B) pH dependence of the fluorescence decrease, ΔF_{\max} , in the absence (●) and presence (○) of 100 μM K⁺. The data were fit with a Hill function, and a pK of 6.8 ± 0.2 ($n = 1.1 \pm 0.4$) was found in the presence of K⁺. On the other hand, the fluorescence decrease was pH-independent in the absence of K⁺ with an average amplitude of -0.19 ± 0.01 .

$$\lambda = 2.2 \times 10^9 \times 10^{-\text{pH}} \quad (5)$$

The ATP release rate constant varies between 2200 s⁻¹ (pH 6) and 22 s⁻¹ (pH 8). The rate constant of the rate-limiting transition step in these experiments is on the order of 1.5 s⁻¹ at pH 8 (Figure 5A), which is in the most unfavorable case still \sim 15 times lower than that of the ATP release process. Therefore, the effect of the pH-dependent ATP release kinetics on the conformational transition process of KdpFABC may be neglected in the pH range covered in the experiments.

Temperature Dependence. Besides structural and kinetic properties, another important aspect in understanding transport performed by ion pumps is the energetics of the transport. One approach to gaining insight into the energetics of the KdpFABC complex is the temperature dependence of enzyme activity and transport function. The malachite green activity assay of the KdpFABC complex solubilized in Aminoxyde WS-35 was performed at different temperatures to determine the activation energy of the ATPase activity. The samples were incubated at temperatures between 6 and 40 °C for 30 min. At higher temperatures (>40 °C), the enzyme activity showed a decrease, probably caused by the denaturation of the KdpFABC complex. The enzyme activity, A , was determined as the

amount of inorganic phosphate released by ATP hydrolysis of the detergent-solubilized KdpFABC complex in a buffer containing 50 mM Tris-HCl, 2 mM MgCl₂ (pH 7.8), 0.33 mM ATP, and 0.2% (w/v) Aminoxyde WS-35 in the nominal absence and presence of (saturating) 100 μM KCl. Three measurements were performed at each temperature, and the average ATPase activity was calculated. To determine the activation energy, E_A , according to the Arrhenius equation, the logarithm of the activity, $\ln A$, was plotted versus reciprocal temperature [Figure 6 (●)]. The data exhibited a bend at $27 \pm$

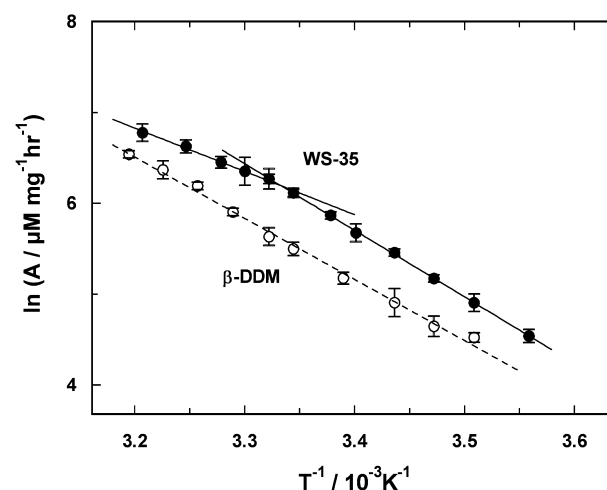


Figure 6. Temperature-dependent ATPase activity of the solubilized KdpFABC complex in Aminoxyde WS-35 and β -DDM determined by the malachite green assay. The ATPase activities are represented as Arrhenius plots, and data are fit with a straight regression line. For KdpFABC solubilized in Aminoxyde WS-35, two activation energies were found: $E_{A,1} = 39.6 \pm 1.6$ kJ/mol at higher temperatures, and $E_{A,2} = 60.9 \pm 0.5$ kJ/mol at lower temperatures (●). For KdpFABC solubilized in β -DDM, the determined activation energy (E_A) was 56.0 ± 1.4 kJ/mol (○).

1 °C, and both parts could be fit with a straight regression line. The obtained activation energies were 39.6 ± 1.6 kJ/mol in the higher-temperature range ($E_{A,1}$) and 60.9 ± 0.5 kJ/mol in the lower-temperature range ($E_{A,2}$). Corresponding measurements were performed with β -DDM-solubilized KdpFABC under the same conditions, but no bend could be detected in the Arrhenius plot. In this detergent, the enzyme activity was lower than in Aminoxyde WS-35 (as reported previously¹⁸), and the activation energy was found to be 56.0 ± 1.4 kJ/mol [Figure 6 (○)]. Bends in the Arrhenius plots have previously been described in cases of many other ion pumps and channels and are generally interpreted as an indication of a phase transition in the surrounding lipid and/or detergent phase.³⁵ Contrary to that of Aminoxyde WS-35, the temperature dependence of the β -DDM-solubilized enzyme's activity indicates that no change of the hydrocarbon chain mobility (lipid fluidity) occurs in the presence of this detergent in the temperature range covered by the experiments.

To investigate the effect of temperature on the rate constant of the conformational transition of KdpFABC solubilized in Aminoxyde WS-35, time-resolved RH421 fluorescence experiments were performed at different temperatures and saturating ATP concentrations. Upon the release of ATP from 300 μM caged ATP, the fluorescence decreases were monitored in the absence and presence of 100 μM K⁺ at pH 7.8 between 8.5 and

37 °C (Figure 7A). At each temperature, at least three measurements were performed, and the average fluorescence

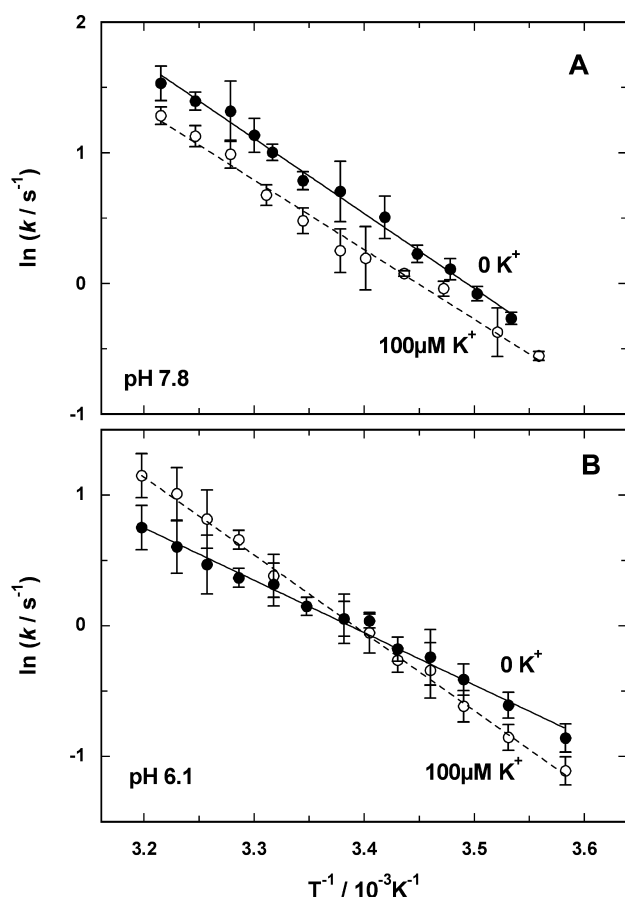
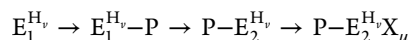


Figure 7. Temperature dependence of the rate constants of the conformational transition. The rate constants, k , determined from ATP concentration jump experiments are represented as Arrhenius plots, and data are fit with a regression line. (A) Experiments performed at pH 7.8 in the absence and presence of 100 μM K⁺. The following activation energies were determined: $E_A(0\text{ K}^+) = 48 \pm 1$ kJ/mol, and $E_A(100\text{ μM K}^+) = 44 \pm 2$ kJ/mol. (B) At pH 6.1, the following activation energies were determined: $E_A(0\text{ K}^+) = 33 \pm 1$ kJ/mol, and $E_A(100\text{ μM K}^+) = 50 \pm 1$ kJ/mol.

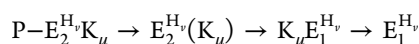
signal was fit with a single-exponential function to obtain the rate constant of the conformational transition. An Arrhenius plot of the data was constructed and fit with a regression line. The activation energies (E_A) were found to be 48 ± 1 kJ/mol in the absence of K⁺ and 44 ± 2 kJ/mol in the presence of 100 μM K⁺. These results suggest that the activation energy is not significantly dependent on the free K⁺ concentration at pH 7.8. To investigate the effect of protons, experiments were performed under the same conditions at pH 6.1 (Figure 7B). At this lower pH, the activation energy (E_A) was found to be 33 ± 1 kJ/mol in the absence of K⁺ and 50 ± 1 kJ/mol in the presence of 100 μM K⁺.

DISCUSSION

Time-resolved experiments provide additional information about the kinetic properties of the KdpFABC reaction cycle. In ATP concentration jump experiments, the following sequence of reaction steps is triggered according to the recently proposed Post-Albers cycle (Figure 1C)



In the last reaction step, the letter X stands for either K⁺, as the physiological substrate, or H⁺, as a low-affinity congener that comes into play in the absence of K⁺. At saturating ATP and K⁺ concentrations, the rate-determining step is supposed to be the conformational transition ($E_1^{H_v}-P \rightarrow P-E_2^{H_v}$). This claim is supported by the fact that the activation energy of the detected process, E_A , is >30 kJ/mol under all experimental conditions (Figure 7). This is a clear indication of a conformational reorganization of a protein. The fluorescence decrease observed upon photorelease of ATP (Figure 2A) results from the binding of positive charge inside the membrane domain of the KdpFABC complex. In the presence of K⁺, the pumps work under turnover conditions and proceed through the Post-Albers cycle, and therefore, the reaction sequence described above is continued



However, the K⁺ release reaction, $K_\mu E_1^{H_v} \rightarrow E_1^{H_v}$, must be delayed by a preceding, rate-limiting reaction step because no significant fluorescence increase was observed, which would be the result of the loss of positive charge inside the membrane domain.

When the concentration of released ATP is reduced, the rate limitation is shifted from the conformational transition to the ATP binding step (Figure 2B). A half-saturating ATP concentration ($K_{1/2} \approx 70\text{ μM}$) was determined at pH 6.1 and 7.8, showing no significant pH dependence. In contrast, the rate constant of the detected process at pH 6.1 was larger by a factor of 1.4 than that with the data at pH 7.8. This was true also at the saturating ATP concentration, and therefore, the pH dependence may be assigned to the conformational transition (see below).

Origin of the RH421 Fluorescence Change. The recorded fluorescence decrease could be fueled by two different electrogenic processes. The first process is the electrogenic binding of nontransported protons on the cytoplasmic side ($E_1 \rightarrow E_1^{H_v}$), and the second process comprises ion binding to the ion transport sites in the P-E₂ conformation ($P-E_2^{H_v} \rightarrow P-E_2^{H_v}X_\mu$). Both mechanisms are diffusion-controlled processes that are orders of magnitude faster than the observed process with a time constant of ~600 ms. Binding and release of protons to the nontransporting sites may be assumed to be in equilibrium if the pH is not changed and, therefore, may be neglected. A fluorescence decrease was observed under all experimental conditions, and this observation confirms that two important features of the ion pump are valid after the ATP-induced phosphorylation and the conformational transition. (1) No protons are released after the transition into the P-E₂ state, which would have generated a fluorescence increase, and (2) cations are bound after the conformational transition to the P-E₂ state, either K⁺ or H⁺ in the absence of K⁺.

Mechanism of K⁺ Transport. When these experiments were performed at pH 7.8, it was found that the observed rate constant, k , had an average value of $\sim 1.7\text{ s}^{-1}$, and it was independent of the potassium concentration, although the K⁺ concentration was varied between 0 and 500 μM (Figure 3). The constant value of the rate constant further implies that K⁺ binding is not the rate-limiting process even at low concentrations [i.e., below the $K_{1/2}$ of 6 μM (Figure 4)], unlike ATP binding (Figure 2B). This fact shows that K⁺ binding does not occur before enzyme phosphorylation or the

conformational transition. The fluorescence amplitude was, however, K^+ -dependent (Figure 4A) and reflects the fraction of KdpFABC complexes that are able to participate in the ATP-triggered reaction sequence and K^+ binding. This can be explained on the basis of the Post–Albers cycle shown in Figure 1C. When the ion pumps are equilibrated at a given K^+ concentration in the buffer before the measurement is performed (as in the experiments analyzed in Figure 4), the amount of K^+ determines the fraction of pumps that can proceed from the $P-E_2$ state through the dephosphorylation half-cycle [$P-E_2^{H_v} + \mu K^+_{ext} \rightarrow P-E_2^{H_v} K_\mu \rightarrow P-E_2^{H_v} (K_\mu) \rightarrow K_\mu E_1^{H_v} \rightarrow E_1^{H_v} + \mu K^+_{cyl}$]. The higher the K^+ concentration, the more pumps are converted to the E_1 conformation, have the K^+ released, and are ready to be phosphorylated. By binding K^+ ions after phosphorylation, they contribute to the detected fluorescence change. According to eq 3, the initial slope of the time-dependent fluorescence decrease (Figure 4B) is proportional to the number of pumps, N_p , in E_1 . The half-saturating K^+ concentration agrees with the value obtained in equilibrium titration experiments.¹⁸ All these findings indicate that K^+ ions bind in the $P-E_2$ conformation of the pump and support the proposal that K^+ ions are transported into the cell in the dephosphorylation half-cycle of the Post–Albers scheme (Figure 1C).

Effect of Protons on the Transport Mechanism. The role of protons and their interaction with the KdpFABC pump are complex, and so far, at least three different mechanisms have been proposed.¹⁸ (1) Protons act as a functional substrate that is bound electrogenically to sites inside the membrane domain of the protein. They are not translocated across the membrane but are necessary to permit (or at least promote) the ATP-hydrolyzing half-cycle of the ion pump. (2) H^+ ions are able to bind to the K^+ binding sites and act as a weak competitor of the transported K^+ and are translocated as congeners in the absence of K^+ . (3) H^+ ions bind to a so far unidentified allosteric site (or sites) and affect the enzyme activity and/or the coupling between the KdpB and KdpA subunits. These three mechanisms cannot easily be discriminated by the experimental techniques available; therefore, the observed pH dependencies of the pump functions have to be analyzed carefully to discriminate and assign the effects correctly.

In Figure 5, the pH dependencies of the rate constant, k , and the fluorescence amplitude are shown. In the presence of saturating $100 \mu M K^+$, the speed of the rate-limiting process increased by a factor of ~ 3 when the pH was reduced from 8.6 to 6.15. This observation fits well with the results of the ATP concentration dependence at pH 6.1 and 7.8 (Figure 2B), in which the higher rate constant at pH 6.1 could be assigned to the faster conformational transition ($E_1^{H_v}-P \rightarrow P-E_2^{H_v}$). A likely explanation is that the binding equilibrium [$\nu H^+ + E_1 \leftrightarrow E_1^{H_v}$ (Figure 1C)] is shifted to the right side at low pH, forming the functional state that is ready to undergo enzyme phosphorylation and the conformational transition to the $P-E_2^{H_v}$ state. At higher pH values, the probability of the functional sites being occupied is reduced and a delay occurs until all sites are filled and allow enzyme phosphorylation. This leads to an apparently lower rate constant of the conformational transition with an increasing pH.

Concurrently with the pH-dependent increase in k , the associated amplitude of the fluorescence decrease was reduced by a factor of ~ 4 between pH 7.8 and 6.2 in the presence of a saturating K^+ concentration (Figure 5B). This result indicates

that only a small number of pump molecules contributed at low pH. Because the K^+ concentration was saturating, the equilibrium between the $P-E_2$ state and the E_1 state was shifted strongly to the E_1 conformation because of K^+ transport. A possible mechanism of the inhibition of active pump molecules is a “back-binding” of H^+ to the binding sites from which K^+ was released, trapping a majority of pump molecules in the $H_\mu E_1^{H_v}$ state. This (unphysiological) side reaction would also explain the pH dependence of the enzyme activity of the KdpFABC complex that was reduced by a factor of >3 when the pH was lowered from 8.5 to 6.¹⁸

In the absence of K^+ , a nonlinear behavior of k was observed (Figure 5A). At high pH values (>7.5), the same low value was found as in the presence of $100 \mu M K^+$, which may be attributed to the lack of protons that fill the functional sites in $E_1^{H_v}$ (see above). In contrast to the high- K^+ concentration condition, the amplitude of the fluorescence change was extremely small in the whole pH range covered by the experiments (Figure 5B). The most probable explanation is that because of the weak binding of H^+ to the transport sites most of the pumps are trapped in the $P-E_2$ conformation. Therefore, only a minor fraction of pumps contribute to the conformational transition upon the ATP concentration jump in these experiments, and because the pK values in the E_1 and $P-E_2$ conformations are similar,¹⁸ the number of bound protons is not significantly different in these conformations, which further decreased the detected fluorescence change.

At low pH and in the presence of a saturating K^+ concentration, most of the pumps are in the E_1 conformation, have protons bound to the functional site, and can undergo the unrestricted $E_1^{H_v}-P \rightarrow P-E_2^{H_v}$ conformational transition (Figure 5A). However, because of the back-binding of protons mentioned above, only a small number of pumps contribute to the detected fluorescence signal, because most of the pumps have the same number of charges in their binding sites before and after the transition. Therefore, the amplitude of the fluorescence decrease is small (Figure 5B) as well as the initial slope (Figure 4B).

The complex pH dependence of the observed rate constant in the absence of K^+ (Figure 5A) can be explained by the role of H^+ as a weak congener. The low rate constant in the high-pH range is caused, as in the presence of K^+ (see above), by the empty functional sites whose necessary occupation apparently slows the progress through the reaction sequence. At low pH values, the rate constants are similarly low (Figure 5A). This reduction must be caused obviously by a step that is faster in the presence of K^+ , i.e., steps in which K^+ is bound to the KdpFABC complex. Therefore, only steps that are in the dephosphorylation half-cycle [$P-E_2^{H_v} K_\mu \rightarrow E_2^{H_v} (K_\mu) \rightarrow K_\mu E_1^{H_v}$] have to be considered. A rate-limiting slow transition through this sequence will fill up the “reservoir” of pump molecules in the E_1 conformation so slowly that upon the ATP concentration jump the fluorescence change is small (as in the case of H^+ back-binding) and the apparent rate constant of the fluorescence decrease becomes very low. When the pH dependence of the enzyme activity was determined in the absence of K^+ , a similar reduction by a factor of ~ 3 was found between pH 8.5 and 6.¹⁸ In the pH range of 7.0–7.5, however, the rate constant is enhanced in the absence of K^+ . This indicates that the number of bound H^+ ions affects the partial reaction mentioned above. The steep pH dependence around pH ~ 7 in Figure 5A, with a Hill coefficient of ~ 4 , points to the cooperative binding of a number of protons. An evident

explanation could be that more H^+ ions are able to bind than K^+ ions. This is supported by the finding that in steady-state titration experiments at pH 6 (in the absence of K^+) more protons were bound than when the sites were saturated with K^+ .¹⁸

In summary, the experimental findings can be explained by a twofold action of H^+ . (1) There are functional sites in which protons are not transported that have to be, however, occupied to promote enzyme phosphorylation and the conformational transition from E_1 to E_2 , in which K^+ ions are bound from the extracellular medium and transported consecutively into the cytoplasm. (2) A competition of H^+ with K^+ at the ion binding sites for K^+ transport in the E_1 conformation leads to H^+ back-binding that slows the progress through the pump cycle at unphysiologically low pH values. In the absence of K^+ , protons are able to bind as congeners in the $P-E_2$ state and promote the progress through the dephosphorylation half-cycle. At low pH values (<7), surplus H^+ ions bind and compete in the $P-E_2$ state, thus inhibiting the progress through the pump cycle. Both action principles can explain all presented experiments, and so far, the initially proposed unspecific, allosteric proton binding sites seem not be needed as a regulatory mechanism of the function of the KdpFABC complex in the studied reaction sequences.

Effects on the Activation Energy. The temperature-dependent ATPase activity of the solubilized KdpFABC complex in both Aminoxide WS-35 and β -DDM (Figure 6) was used to determine the activation energy, E_A , of the rate-limiting step of the ATP-triggered reaction sequence. When the KdpFABC complex was solubilized in Aminoxide WS-35, E_A showed a bend at $\sim 27^\circ\text{C}$, in contrast to the enzyme solubilized in β -DDM. The overall protein flexibility may be essential for the enzymatic activity and is affected by the lipid/detergent environment. Therefore, the biphasic behavior observed in the case of Aminoxide WS-35 could be related to some minor yet unknown component(s) of this detergent mixture. This component may mimic the role of a functional lipid that got lost during the isolation and purification process of the KdpFABC complex. Functionally essential lipids bound to a P-type ATPase have been identified in the case of the Na,K-ATPase.³⁶ Previously published results revealed that only the unspecified mixture of detergents, Aminoxide WS-35, provided a functional complex with a $K_{1/2}(K^+)$ of $6.5\ \mu\text{M}$ that is on the same order of magnitude as the values reported for the ion pump in its native environment.³⁷ The KdpFABC complex purified with other detergents, including β -DDM, resulted in lower ATPase activities and K^+ binding affinities; the latter were more significantly affected.¹⁸ The biphasic behavior, with activation energies of $39.6 \pm 1.6\ \text{kJ/mol}$ at higher temperatures ($E_{A,1}$) and $60.9 \pm 0.5\ \text{kJ/mol}$ at lower temperatures ($E_{A,2}$), may be related to the specific component of Aminoxide WS-35 that is crucial for proper enzyme function. Because of a phase transition, its interaction with the KdpFABC complex is modified and thus leads to a greater energy expenditure in the lower-temperature range where this component is assumed to be in a less flexible phase. The mechanism by which this specific component interacts could not be identified, except for the fact that it does not affect the phosphorylation half-cycle because the respective partial reaction exhibits no bend (Figure 7).

The activation energies were not significantly different in the presence of $100\ \mu\text{M}\ K^+$, independent of pH, or in the absence of K^+ at pH 7.8. This is in agreement with the presented

concept that in all three cases the rate-limiting step is the conformational transition ($E_1^{H_3}-P \rightarrow P-E_2^{H_3}$). In the absence of K^+ and at low pH values, however, the dephosphorylation half-cycle becomes rate-limiting [$P-E_2^{H_3}H_\mu \rightarrow E_2^{H_3}(H_\mu) \rightarrow H_\mu E_1^{H_3}$], as discussed above, and the conformational transition in this partial reaction would be an appropriate candidate, because a value of $33\ \text{kJ/mol}$ bears evidence of major conformational rearrangements in the protein structure.

Mechanistic Implications and Proposed Post-Albers Reaction Cycle. The presented experiments and their analysis confirm the recently proposed Post-Albers cycle of the KdpFABC complex.¹⁸ A proposed scheme is outlined in Figure 8. The fluorescence changes observed upon addition of

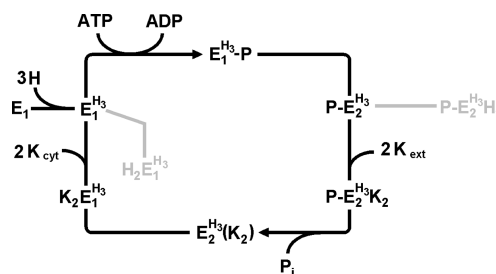


Figure 8. Post-Albers model for the KdpFABC complex proposed on the basis of the presented results and experimentally determined stoichiometric factors (cf. Figure 1C) of $\nu = 3$ and $\mu = 2$ for H^+ and K^+ , respectively. The additions in light gray indicate additional, inhibitory reaction steps at low pH values and/or in the absence of K^+ .

satulating concentrations of K^+ and H^+ were determined to be in a ratio of $2/3$.¹⁸ This suggests a stoichiometry of two K^+ ions bound in the transport sites and three H^+ ions bound to the so-called functional sites that are located inside the membrane dielectric. Occupation of these functional sites is a prerequisite for efficient phosphorylation of the KdpFABC complex by ATP. The available results do not allow the claim that empty functional sites inactivate phosphorylation completely; however, if phosphorylation is possible with empty functional sites, the rate must be significantly reduced. In Figure 8, binding of H^+ is assigned to the E_1 state. In principle, binding or release of these functional H^+ ions could occur also in other states, but the access pathway to these sites remains on the same side of the membrane because no transport of protons across the membrane can be detected.

In the $P-E_2$ conformation, two K^+ ions bind from the extracellular aqueous phase to the transport sites. Occupation of the sites triggers enzyme dephosphorylation, followed by K^+ occlusion and subsequent conformational transition back to the E_1 conformation. The latter step seems to be the rate-limiting step in the dephosphorylation half-cycle, because the low fluorescence level obtained after starting pump turnover by addition of ATP indicates that a state with both K^+ ions in the binding sites is maintained. In the absence of K^+ , congeners are able to replace K^+ in the transport sites, although with significantly lower affinity and efficiency.^{15–18} This property of the KdpFABC complex is not included in Figure 8.

Under unphysiological conditions, i.e., at low pH values (<6.5) or in the absence of K^+ , additional, mostly inhibitory side reactions were detected. Because of the lower affinity for K^+ in the E_1 conformation, the binding sites are empty and H^+ binding takes place at low pH values. This condition traps the pumps in the $H_2E_1^{H_3}$ state and prevents (or limits)

phosphorylation by ATP. Another inhibitory side reaction was observed in the absence of K^+ in the $P-E_2$ conformation ($P-E_2^{H_1} \rightarrow P-E_2^{H_2}$). The number of bound H^+ ions must be $\kappa > 2$, to inhibit the propagation through the turnover with H^+ as a congener. This assumption is in agreement with the finding from titration experiments in the $P-E_2$ state,¹⁸ in which it was found that more H^+ ions than K^+ ions can be bound.

In summary, we can conclude that the pump cycle of the KdpFABC complex under physiological conditions resembles that of the Na,K-ATPase or H,K-ATPase, each of which also translocates two K^+ ions into the cytoplasm in the dephosphorylation half-cycle. In the ATP-dependent half-cycle of KdpFABC, no ions are translocated across the membrane, but three H^+ ions have to be bound to the functional sites in the membrane domain to promote enzyme phosphorylation. So far, we cannot conclusively identify the subunit in which these sites are present. They could be located in the KdpA subunit in analogy to a regulatory role that protons have in the gating of the KcsA potassium channel. This proposal is supported by a recent study³⁷ of the bacterial KcsA channel, from which it was concluded that binding of protons to amino acids from the intracellular side of the K^+ channel leads to an open gated conformation. Possibly, a related mechanism may occur in the case of the KdpA subunit, in which protons affect the state of the occlusion gate that has to be in a distinct position to promote the conformational transition from E_1 to E_2 . An alternative explanation would be H^+ binding sites in the KdpB subunit or specifically at the interface between both subunits where the energetic coupling is performed. Further investigations are necessary to shed light on this mechanism.

AUTHOR INFORMATION

Corresponding Author

*Phone: +49 7531 882253. Fax: +49 7531 883183. E-mail: h-j.apell@uni-konstanz.de.

Funding

We gratefully acknowledge funding from the Konstanz Research School Chemical Biology, University of Konstanz, Germany, and the University of Konstanz (AFF 4/68).

Notes

The authors declare no competing financial interests.

ABBREVIATIONS

RH421, *N*-(4-sulfobutyl)-4-{4-[4-(dipentylamino)phenyl]-butadienyl}pyridinium, inner salt; β -DDM, *n*-dodecyl β -D-maltoside; NPE-caged ATP, adenosine 5'-triphosphate P3-[1-(2-nitrophenyl)ethyl ester] disodium salt.

REFERENCES

- (1) Chan, H., Babayan, V., Blyumin, E., Gandhi, C., Hak, K., Harake, D., Kumar, K., Lee, P., Li, T. T., Liu, H. Y., Lo, T. C., Meyer, C. J., Stanford, S., Zamora, K. S., and Saier, M. H., Jr. (2010) The p-type ATPase superfamily. *J. Mol. Microbiol. Biotechnol.* 19, 5–104.
- (2) Möller, J. V., Juul, B., and le Maire, M. (1996) Structural organization, ion transport, and energy transduction of P-type ATPases. *Biochim. Biophys. Acta* 1286, 1–51.
- (3) Toyoshima, C., Nakasako, M., Nomura, H., and Ogawa, H. (2000) Crystal structure of the calcium pump of sarcoplasmic reticulum at 2.6 Å resolution. *Nature* 405, 647–655.
- (4) Toyoshima, C., Nomura, H., and Sugita, Y. (2003) Crystal structures of Ca^{2+} -ATPase in various physiological states. *Ann. N.Y. Acad. Sci.* 986, 1–8.
- (5) Olesen, C., Sørensen, T., Nielsen, R. C., Möller, J. V., and Nissen, P. (2004) Dephosphorylation of the calcium pump coupled to counterion occlusion. *Science* 306, 2251–2255.
- (6) Sørensen, T. L., Olesen, C., Jensen, A. M., Möller, J. V., and Nissen, P. (2006) Crystals of sarcoplasmic reticulum Ca^{2+} -ATPase. *J. Biotechnol.* 124, 704–716.
- (7) Bramkamp, M., Altendorf, K., and Greie, J. C. (2007) Common patterns and unique features of P-type ATPases: A comparative view on the KdpFABC complex from *Escherichia coli*. *Mol. Membr. Biol.* 24, 375–386.
- (8) van der Laan, M., Gassel, M., and Altendorf, K. (2002) Characterization of amino acid substitutions in KdpA, the K^+ -binding and -translocating subunit of the KdpFABC complex of *Escherichia coli*. *J. Bacteriol.* 184, 5491–5494.
- (9) Durell, S. R., Bakker, E. P., and Guy, H. R. (2000) Does the KdpA subunit from the high affinity K^+ -translocating P-type KDP-ATPase have a structure similar to that of K^+ channels? *Biophys. J.* 78, 188–199.
- (10) Becker, D., Fendler, K., Altendorf, K., and Greie, J. C. (2007) The conserved dipole in transmembrane helix 5 of KdpB in the *Escherichia coli* KdpFABC P-type ATPase is crucial for coupling and the electrogenic K^+ -translocation step. *Biochemistry* 46, 13920–13928.
- (11) Ahnert, F., Schmid, R., Altendorf, K., and Greie, J. C. (2006) ATP binding properties of the soluble part of the KdpC subunit from the *Escherichia coli* K^+ -transporting KdpFABC P-type ATPase. *Biochemistry* 45, 11038–11046.
- (12) Irzik, K., Pfrotzschner, J., Goss, T., Ahnert, F., Haupt, M., and Greie, J. C. (2011) The KdpC subunit of the *Escherichia coli* K^+ -transporting KdpB P-type ATPase acts as a catalytic chaperone. *FEBS J.* 278, 3041–3053.
- (13) Gassel, M., Mollenkamp, T., Puppe, W., and Altendorf, K. (1999) The KdpF subunit is part of the K^+ -translocating Kdp complex of *Escherichia coli* and is responsible for stabilization of the complex in vitro. *J. Biol. Chem.* 274, 37901–37907.
- (14) Bramkamp, M., and Altendorf, K. (2005) Single amino acid substitution in the putative transmembrane helix V in KdpB of the KdpFABC complex of *Escherichia coli* uncouples ATPase activity and ion transport. *Biochemistry* 44, 8260–8266.
- (15) Schrader, M., Fendler, K., Bamberg, E., Gassel, M., Epstein, W., Altendorf, K., and Drose, S. (2000) Replacement of glycine 232 by aspartic acid in the KdpA subunit broadens the ion specificity of the K^+ -translocating KdpFABC complex. *Biophys. J.* 79, 802–813.
- (16) Buurman, E. T., Kim, K. T., and Epstein, W. (1995) Genetic evidence for two sequentially occupied K^+ binding sites in the Kdp transport ATPase. *J. Biol. Chem.* 270, 6678–6685.
- (17) Bertrand, J., Altendorf, K., and Bramkamp, M. (2004) Amino acid substitutions in putative selectivity filter regions III and IV in KdpA alter ion selectivity of the KdpFABC complex from *Escherichia coli*. *J. Bacteriol.* 186, 5519–5522.
- (18) Damjanovic, B., Weber, A., Potschies, M., Greie, J. C., and Apell, H. J. (2013) Mechanistic analysis of the pump cycle of the KdpFABC P-type ATPase. *Biochemistry* 52, 5563–5576.
- (19) Bühler, R., Stürmer, W., Apell, H.-J., and Längler, P. (1991) Charge translocation by the Na,K-pump: I. Kinetics of local field changes studied by time-resolved fluorescence measurements. *J. Membr. Biol.* 121, 141–161.
- (20) McCray, J. A., Herbet, L., Kihara, T., and Trentham, D. R. (1980) A new approach to time-resolved studies of ATP-requiring biological systems; laser flash photolysis of caged ATP. *Proc. Natl. Acad. Sci. U.S.A.* 77, 7237–7241.
- (21) Siebers, A., and Altendorf, K. (1988) The K^+ -translocating Kdp-ATPase from *Escherichia coli*. Purification, enzymatic properties and production of complex- and subunit-specific antisera. *Eur. J. Biochem.* 178, 131–140.
- (22) Heitkamp, T., Kalinowski, R., Bottcher, B., Borsch, M., Altendorf, K., and Greie, J. C. (2008) K^+ -Translocating KdpFABC P-Type ATPase from *Escherichia coli* Acts as a Functional and Structural Dimer. *Biochemistry* 47, 3564–3575.

- (23) Vagin, O., Denevich, S., Munson, K., and Sachs, G. (2002) SCH28080, a K⁺-competitive inhibitor of the gastric H,K-ATPase, binds near the M5–6 luminal loop, preventing K⁺ access to the ion binding domain. *Biochemistry* 41, 12755–12762.
- (24) Stürmer, W., Apell, H.-J., Wuddel, I., and Läuger, P. (1989) Conformational transitions and change translocation by the Na,K pump: Comparison of optical and electrical transients elicited by ATP-concentration jumps. *J. Membr. Biol.* 110, 67–86.
- (25) Cirri, E., Katz, A., Mishra, N. K., Belogus, T., Lifshitz, Y., Garty, H., Karlsh, S. J., and Apell, H. J. (2011) Phospholemman (FXYP1) Raises the Affinity of the Human $\alpha_1\beta_1$ Isoform of Na,K-ATPase for Na Ions. *Biochemistry* 50, 3736–3748.
- (26) Deluca, M., and McElroy, M. D. (1978) Purification and properties of firefly luciferase. *Methods Enzymol.* 57, 3–15.
- (27) Kaplan, J. H., and Hollis, R. J. (1980) External Na dependence of ouabain-sensitive ATP:ADP exchange initiated by photolysis of intracellular caged-ATP in human red cell ghosts. *Nature* 288, 587–589.
- (28) Apell, H.-J., Roudna, M., Corrie, J. E., and Trentham, D. R. (1996) Kinetics of the phosphorylation of Na,K-ATPase by inorganic phosphate detected by a fluorescence method. *Biochemistry* 35, 10922–10930.
- (29) Fendler, K., Drose, S., Altendorf, K., and Bamberg, E. (1996) Electrogenic K⁺ transport by the Kdp-ATPase of *Escherichia coli*. *Biochemistry* 35, 8009–8017.
- (30) Siebers, A., and Altendorf, K. (1989) Characterization of the phosphorylated intermediate of the K⁺-translocating Kdp-ATPase from *Escherichia coli*. *J. Biol. Chem.* 264, 5831–5838.
- (31) Rhoads, D. B., Waters, F. B., and Epstein, W. (1976) Cation transport in *Escherichia coli*. VIII. Potassium transport mutants. *J. Gen. Physiol.* 67, 325–341.
- (32) Borlinghaus, R., and Apell, H.-J. (1988) Current transients generated by the Na⁺/K⁺-ATPase after an ATP concentration jump: Dependence on sodium and ATP concentration. *Biochim. Biophys. Acta* 939, 197–206.
- (33) McCray, J. A., and Trentham, D. R. (1989) Properties and uses of photoreactive caged compounds. *Annu. Rev. Biophys. Biophys. Chem.* 18, 239–270.
- (34) Borlinghaus, R., Apell, H.-J., and Läuger, P. (1987) Fast charge translocations associated with partial reactions of the Na,K-pump: I. Current and voltage transients after photochemical release of ATP. *J. Membr. Biol.* 97, 161–178.
- (35) Harmel, N., and Apell, H. J. (2006) Palytoxin-induced effects on partial reactions of the Na,K-ATPase. *J. Gen. Physiol.* 128, 103–118.
- (36) Mishra, N. K., Peleg, Y., Cirri, E., Belogus, T., Lifshitz, Y., Voelker, D. R., Apell, H. J., Garty, H., and Karlsh, S. J. (2011) FXYP proteins stabilize Na,K-ATPase: Amplification of specific phosphatidylserine-protein interactions. *J. Biol. Chem.* 286, 9699–9712.
- (37) Posson, D. J., Thompson, A. N., McCoy, J. G., and Nimigeon, C. M. (2013) Molecular interactions involved in proton-dependent gating in KcsA potassium channels. *J. Gen. Physiol.* 142, 613–624.